Electrochimica Acta 464 (2023) 142874

Contents lists available at ScienceDirect

Electrochimica Acta

journal homepage: www.journals.elsevier.com/electrochimica-acta

# Combination of solid polymer electrolytes and lithiophilic zinc for improved plating/stripping efficiency in anode-free lithium metal solid-state batteries

Luca Bertoli [a,b], Sophia Bloch [b], Edvin Andersson [b], Luca Magagnin [a], Daniel Brandell [b], Jonas Mindemark [b,*]

[a] Dipartimento di Chimica, Materiali e Ingegneria Chimica "Giulio Natta", Politecnico di Milano, Via Luigi Mancinelli 7, Milan 20131, Italy
[b] Department of Chemistry – Ångström Laboratory, Uppsala University, Box 538, SE-751 21 Uppsala, Sweden

ARTICLE INFO

*Keywords:*
Anode-free batteries
Solid polymer electrolytes
Li-metal batteries
Lithiophilic metals
Zinc triflate

ABSTRACT

Anode-free lithium metal batteries and solid-state batteries represent some of the most promising alternatives to the current Li-ion technology. The possibility to reach high energy density, due to the exploitation of Li-metal plating/stripping and the elimination of excess anode material, motivate the interest at both academic and industrial levels. Despite these favourable properties, the use of Li-metal has always been extremely challenging and inefficient. This becomes particularly relevant in anode-free systems where no excess of lithium is introduced in the cell. The efficiency and quality of the deposition process is therefore of utmost importance. To optimize the Li-metal plating process, a combination of solid polymer electrolytes and a lithiophilic metal is applied herein, using *in situ* deposition of a zinc interlayer from a PEO-based SPE to modify the Cu current collector. Improvements in specific capacity, coulombic efficiency and cyclability with the addition of zinc as lithiophilic metal is verified in full anode-free solid-state Li-batteries, while plating/stripping in half-cell configuration provides additional insights into the relevant mechanisms. The exploitation of the *in situ* deposited lithiophilic layer reveals an innovative and practical optimization strategy for the future of anode-free solid-state batteries.

## 1. Introduction

Li-ion batteries constitute an essential technology for efficient energy storage and they are indeed heavily employed to power portable devices, electric vehicles and much other "intelligent" technology [1]. This is mainly due to their good balance between gravimetric and volumetric energy density and the optimal reversibility and efficiency of the electrochemical process [2]. Despite these great advantages, a drastic increase in energy density is still desired, especially to boost the mileage of electric vehicles or for the employment of more dividing applications (heavy vehicles, aviation, etc.). Moreover, Li-ion batteries face some other challenges and risks to be addressed in terms of sustainability, safety and performance [1]. Finding improved alternatives to Li-ion batteries is therefore a critical challenge for the scientific community.

In this regard, Li-metal batteries offer higher energy density and are seen as promising candidates. The Li metal anode has a theoretical specific capacity of 3862 mAh $g^{-1}$, some ten times higher than graphite (372 mAh $g^{-1}$) and an electrode potential which is the lowest among all the elements. Anode-free lithium batteries (AFLBs), which also rely on the Li-metal plating/stripping reaction, could reach even higher volumetric and gravimetric energy density have potentially even higher energy density by removing also the Li-metal anode from the cell; by around 50% compared to Li-ion batteries [3].

Batteries relying on Li-metal as the anode material have been widely studied at the research level, but commercialization of the technology has mainly occurred as primary batteries, with very few exceptions. The main reason is that the plating reaction (i.e. the charging phase) of Li spontaneously takes place by uneven deposition of the Li layer, forming dendritic structures that may cause short-circuits, excessive side reactions, loss of capacity and failure of the device. For AFLBs, removing the presence of any excess of metallic lithium at the anode causes this effect to be even more amplified and an extremely high coulombic efficiency is therefore required in order not to waste the lithium supplied by the cathode material [4,5].

In order to effectively unlock the full potential of AFLBs, there is a need to optimize the growth of the Li layer in a compact and

* Corresponding author.
*E-mail address:* jonas.mindemark@kemi.uu.se (J. Mindemark).

https://doi.org/10.1016/j.electacta.2023.142874
Received 12 May 2023; Received in revised form 5 July 2023; Accepted 10 July 2023
Available online 11 July 2023

homogeneous way. Among the various strategies that have been proposed in recent years [6–11], solid-state batteries (SSBs) represent a valuable solution. SSBs are nowadays one of the most heavily studied and promising technologies, substituting flammable and toxic liquid electrolytes with all-solid-state counterparts that can be either inorganic, polymeric or a combination of both in a composite [12–16]. In particular, solid polymer electrolytes (SPEs) can guarantee greater control and tunability at the electrode-electrolyte interface, following the surface roughness of the electrode material (or Cu current collector in the case of AFLBs) [17]. Moreover, the improved mechanical properties, compared to the liquid counterpart, make it more difficult for dendrites to grow and to damage the electrolyte [18]. SPEs are therefore promising candidates for AFLBs as they help the Li-metal to grow homogeneously, avoiding dendrites [19–22].

Another useful strategy to optimize the lithium growth in AFLBs is to modify the Cu current collector by means of lithiophilic metals [23,24]. This class of metals (e.g. Sn, Zn, Ag, Au, etc.) are lithium-wettable, meaning that with these metals, Li would nucleate homogeneously on the current collector and preferably grow as a uniform interlayer [25–29]. In contrast, a high overvoltage to nucleation, typical of lithiophobic elements like Cu, lead to the formation of scattered nucleation sites, causing the formation of dendrites [30]. Lithiophilic metals are usually deposited on top of the current collector by advanced deposition techniques (e.g. chemical, thermal, sputtering), in order to control the uniformity and their amount to a few layers [31–34]. These deposition techniques are expensive and slow, and generally poorly suitable to scale-up at the industrial level. An alternative option is to coat the Cu current collector with lithiophilic metal powder in the form of a slurry electrode [35,36]. A lithiophilic metal slurry, despite being a much cheaper and scalable solution, introduces extra steps in the battery manufacturing line and reduces the overall volumetric energy of the battery, a major positive aspect of AFLBs. Another possibility is electrodeposition of lithiophilic metals on top of the Cu current collector, but a high uniformity over large areas is generally difficult on very thin substrates, like Cu [37].

In the present work, the effect of solid polymer electrolytes and lithiophilic metals for optimization of AFLBs are studied together. Polyethylene oxide (PEO) was selected as solid polymer electrolyte host material. Lithiophilic zinc metal salts were introduced in the matrix and their effect on the electrochemical performance was evaluated through full-cell characterization and moreover by employing a specific plating-stripping protocol for anode-free systems.

## 2. Experimental

### 2.1. Polymer electrolyte preparation

Polymer electrolytes were prepared in an Ar-filled glovebox ($H_2O$ < 1 ppm, $O_2$ < 1 ppm). The polymer poly(ethylene oxide) (PEO $M_v \approx$ 2,000,000, Sigma-Aldrich), the $Li^+$salts LiTFSI (BASF) and LiDFOB (Sigma Aldrich) and the lithiophilic metal salts $Zn(OTf)_2$ (TCI) and ZnTFSI (Sigma-Aldrich) were dissolved in anhydrous acetonitrile (Sigma-Aldrich) and stirred overnight before being cast in PTFE molds and vacuum dried in a glovebox. The solvent was completely removed through a carefully optimized drying protocol described elsewhere [38]. The films were hot-pressed at 80 °C and 20 MPa to control their thickness to 100 μm ± 10 μm and punched to ø12 mm and ø15 mm samples for impedance and charge-discharge testing, respectively. The $Li^+$ salts were vacuum dried at 120 °C for 48 h before use. For the nomenclature of the samples, the number after the lithiophilic element (i.e. Zn) represents the weight percentage of the salt with respect to the polymer weight. The $Li^+$ salt content was kept constant at 25 wt% (EO/Li ≈ 26), for all the samples while the lithiophilic metal salt was varied. The notation wt% refers to the percentage relative to the mass of PEO.

### 2.2. Electrodes preparation

$LiFePO_4$ (LFP) electrodes were prepared by ball milling the LFP active material powder (Tobmachine) with carbon black (CB, C65, Imerys) and PEO ($M_v \approx$ 400,000, Sigma-Aldrich) as binder with the ratio LFP/CB/binder = 70:15:15 and using anhydrous acetonitrile as solvent. The electrode slurry was coated on aluminum foil with a doctor blade gap of 150 μm. The electrodes were dried overnight at room temperature, punched and dried in a vacuum oven (Buchi) at 120 °C for 5 h and finally stored in a protected atmosphere inside an Ar-filled glovebox ($H_2O$ < 0.5 ppm, $O_2$ < 0.5 ppm). The active mass loading of the as-prepared electrode was around 1.5 – 2.0 mg $cm^{-2}$.

Copper foil current collectors (30 μm thick) were punched and cleaned with diluted hydrochloric acid (HCl 5%, Sigma Aldrich) to obtain a fresh surface, washed with deionized water and ethanol, carefully dried in a vacuum oven at 60 °C and stored in a protected atmosphere to avoid further oxidation of the surface.

### 2.3. Electrochemical characterization

The ionic conductivity of the polymer electrolytes was studied through electrochemical impedance spectroscopy (EIS). EIS analysis was performed between 10 MHz and 1 Hz applying a single-wave potential perturbation with an amplitude of 10 mV around the OCV, in the temperature range 22–80 °C using a Schlumberger 1260 frequency response analyzer. One day prior to the test, coin cells (CR2025, MTI), containing the films were annealed at 80 °C for 1 h to ensure good contact with the stainless steel blocking electrodes. The bulk resistance of the polymer electrolytes was determined by fitting a Debye circuit using ZView software (Scribner Associates). Coin cells (CR2032, MTI) were assembled as zero-excess anode-free solid-state batteries using a ø13 mm Cu current collector as anode and a ø13 mm LFP electrode as cathode, with the polymer film sandwiched in between. Zero-excess means that the negative/positive electrode capacity ratio (N/P ratio) is equal to zero. Galvanostatic cycling tests were performed with a battery tester equipment (Arbin BT-2043). Constant current cycling tests were performed at 0.1C at a fixed temperature of 60 °C, with an upper and lower cut-off voltage of 4.0 V and 2.7 V, respectively. The cells were allowed to rest at OCV conditions for 10 h at 60 °C prior to testing to ensure good interfacial contact. Plating/stripping tests were performed in coin cells (CR2032), assembled in a half-cell configuration using a Cu current collector as the working electrode and Li-metal as counter electrode with the solid polymer membranes as electrolyte. The plating/stripping protocol was designed to carefully analyze the nucleation of the lithiophilic layer and the coulombic efficiency without any influence from the cathodic material. This was performed at 50 μA $cm^{-2}$ with a fixed plating areal capacity of 0.025 mAh $cm^{-2}$ at 60 °C.

## 3. Results and discussion

PEO was selected as the solid polymer electrolyte host material, combined with LiTFSI as the $Li^+$ charge carrier and lithiophilic zinc in the form of TFSI and triflate salts, being easily accessible and soluble zinc sources. The Zn-salts were dissolved in the polymer solution along with the Li-salt, so that the resulting SPE contained both $Li^+$ and the $Zn^{2+}$ ions of the lithiophilic metal. By having a reduction potential higher than that of Li, the deposition of Zn will occur before the Li plating in the very first charging step, forming a very thin layer controlled by the amount of Zn-salt added to the SPE. Moreover, with Zn having an oxidation potential outside of the operating potential range of the electrode during battery operation, this layer should not be affected by the subsequent charge-discharge cycles. Zn is in this context a particularly effective lithiophilic metal, which can be plated at a potential (−0.76 V vs SHE) between the Li plating/stripping reaction (−3.04 V vs SHE) and conventional Li-battery cathode materials which operate at potential values higher than 0 V vs SHE.

To assess the influence of the lithiophilic metals, PEO-based SPEs were prepared by a solvent casting technique containing a fixed amount (25 wt%) of either LiTFSI or LiDFOB and $Zn(OTf)_2$ (triflate) or ZnTFSI as the source of $Zn^{2+}$ ions. The effect of the triflate-based lithiophilic salts on the ionic conductivity of the PEO:LiTFSI SPE was first analyzed through electrochemical impedance spectroscopy performed at different temperatures, ranging from room temperature to 80 °C. The total ionic conductivities were calculated from the bulk resistance of the impedance data, showing good agreement with previously published results on PEO:LiTFSI systems [39,40]. The ionic conductivity ranged from $10^{-6}$ to $10^{-4}$ S $cm^{-1}$ with increasing temperature, confirming that the lithiophilic metal salt did not have a large effect on the mobility of the other ions in the SPEs (Fig. 1). Through DSC analysis, it was also confirmed that the lithiophilic metal salt did not affect either the $T_g$ or the $T_m$ of the SPEs, which remained almost constant around −33.0 °C and 62 °C, respectively (Figure S1). For the 12.5 wt% $Zn(OTf)_2$ electrolyte, a less remarkable kink is found in the ionic conductivity around $T_m$, although both electrolytes feature this kink at about the same temperature (in line with the similar melting points as determined by DSC). This difference in behavior rather seems to be caused by differences in conduction behavior above and below $T_m$ for these systems. It is possible that due to the high donor number of triflates, the presence of $Zn(OTf)_2$ can also affect $Li^+$ movement and explain the change in temperature dependence observed [41].

In order to test the behavior of the zinc salts on battery cycling, anode-free cells (Cu vs. LFP) were assembled in a coin cell configuration. The PEO electrolyte containing only LiTFSI salt showed generally worse cycling performance (Fig. 2). In particular, the 1st cycle capacity was 82 mAh $g^{-1}$ for the PEO:LiTFSI SPE, while upon addition of $Zn(OTf)_2$ a value as high as 125 mAh $g^{-1}$ for a concentration of lithiophilic salt of 2.5 wt% could be achieved for the same LFP cathode material. The specific capacity of the battery during cycles is highly dependent on the initial coulombic efficiency (ICE), especially when an anode-free configuration is employed. Indeed, as can be seen in Fig. 2, a low ICE is associated to a low initial specific capacity. While the results suggest that the PEO:LiTFSI electrolyte is not a very efficient system in the anode-free configuration, they also clearly indicate a positive effect of the addition of the lithiophilic salt, which is able to increase both the delivered capacity and the coulombic efficiency of the cell. An overall better capacity retention of the battery was achieved, even though the remaining specific capacity after merely 10 cycles was not enough to further continue the characterization. For comparison, an SPE containing LiDFOB salt was produced as an alternative source of $Li^+$ and the effect of ZnTFSI was also analysed in both LiTFSI- and LiDFOB-containing PEO matrices as an alternative $Zn^{2+}$ source. $Zn(OTf)_2$ was found to outperform ZnTFSI in both LiTFSI and LiDFOB systems, and LiDFOB showed less capacity fading than LiTFSI (Fig. S3-S4). These results suggests that TFSI -containing salts may not be the most suitable ones for anode-free systems. It is possible that the TFSI is more prone to decomposition during the SEI formation with respect to other counter ions (e.g. $TfO^-$ and DFOB tested herein) [42].

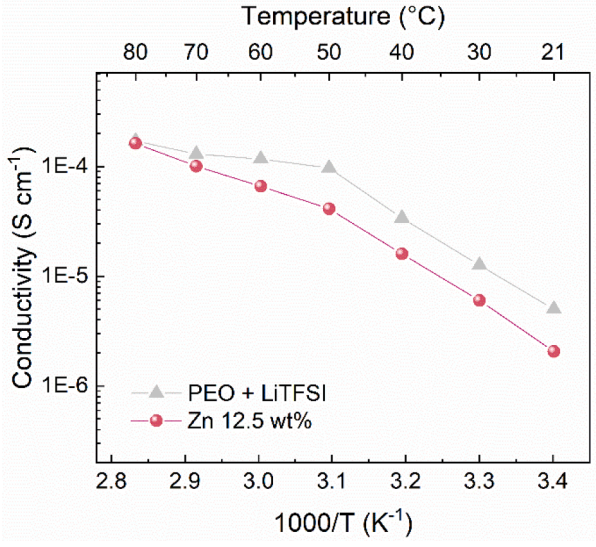


**Fig. 1.** Ionic conductivity as a function of temperature for PEO:LiTFSI and PEO:LiTFSI:$Zn(OTf)_2$ SPEs (LiTFSI concentration fixed at 25 wt% and $Zn(OTf)_2$ concentration of 12.5 wt%).

To have a more clear insight into the effects of using the lithiophilic salt, a plating/stripping protocol involving Cu vs. Li (i.e., half-cells) in a coin cell configuration was introduced. By removing the influence of the cathode material, it is possible to investigate the Li plating/stripping process solely and obtain direct information on the coulombic efficiency, nucleation overpotentials and on the amount of Li-metal deposited. Fig. 3a and b show the very first cycle of the plating/stripping test for different amounts of Zn triflate salt, followed by the first full Li plating/stripping cycle. The deposition of a layer of lithiophilic material, obtained *in situ* during operation, is evident in the first plating cycle, with the appearance of a voltage plateau at around 1.0 V vs $Li^+$/Li. This nucleation and subsequent plating region starting at 1.0 V vs $Li^+$/Li is associated to Zn-metal deposition, which is taking place significantly above the Li plating region that is typically below 0.0 V vs $Li^+$/Li. This plateau shows an increase in capacity as the amount of zinc salt is increased and is most apparent at the highest concentration of $Zn(OTf)_2$ (25 wt%); see Fig. 3b. In this case, the plating capacity of the lithiophilic layer was higher than 0.025 mAh $cm^{-2}$, so the plating curve subsequentially shows some spikes associated to the beginning of another plating cycle, until all the lithiophilic material was deposited.

In this half-cell configuration, it is likely that the lithiophilic salt interacts spontaneously with the Li-metal electrode upon cell assembly. This would explain why a higher amount of Zn-salt was required to obtain comparable performance to the full-cell cycling.

By limiting the upper voltage for the Li stripping, it should be possible to maintain the zinc layer unaffected in the subsequent cycles, since it will not undergo any electrochemical oxidation. As a consequence, the Li plating/stripping reaction will occur on the Zn-modified current collector surface instead of on the bare Cu current collector. Fig. 3c displays the 20th cycle of the plating/stripping protocol for the different applied concentrations of $Zn(OTf)_2$. The effect of Zn was also analyzed through cyclic voltammetry (CV) and linear sweep voltammetry (LSV) in Fig. S2, confirming the presence of peaks associated with the Zn-metal before the Li-nucleation regime, around 1.0 V vs $Li^+$/Li. In Fig. 3c, the lower nucleation overpotential for Zn-containing SPEs demonstrates a better plating of the lithium layer compared to the bare Cu current collector. The bare Cu sample displays a sharp voltage dip and a high nucleation overpotential of around 20 mV during cycling (inset of Fig. 3c), indicative of irregular nucleation sites, mainly responsible for dendrites growth and mossy structures [43]. After the very first cycle, no further plating of the lithiophilic Zn-metal could be seen, demonstrating that the zinc layer deposited at the beginning remains unaffected largely during cycling. Here, it provides an improved coulombic efficiency. Comparing the coulombic efficiencies in the plating/stripping cycles (Fig. 3d), the presence of the lithiophilic salt in the SPE helps achieving higher efficiency values and better stability upon cycling, being around 60% in the PEO:LiTFSI system and around 80% when $Zn(OTf)_2$ is added, for more than 100 cycles. An uncontrolled deposition and dendrite formation for the Zn-free reference PEO:LiTFSI system started to become evident above 100 cycles, as seen from the irregular behavior of the coulombic efficiency in Fig. 3d, likely corresponding to inactive lithium and loss of connection from the current collector. These results from the plating-stripping test are in accordance with the cycling data shown above for the full anode-free solid-state LFP-based battery, confirming a good reliability of the employed half-cell protocol, which also offers additional control and relevant

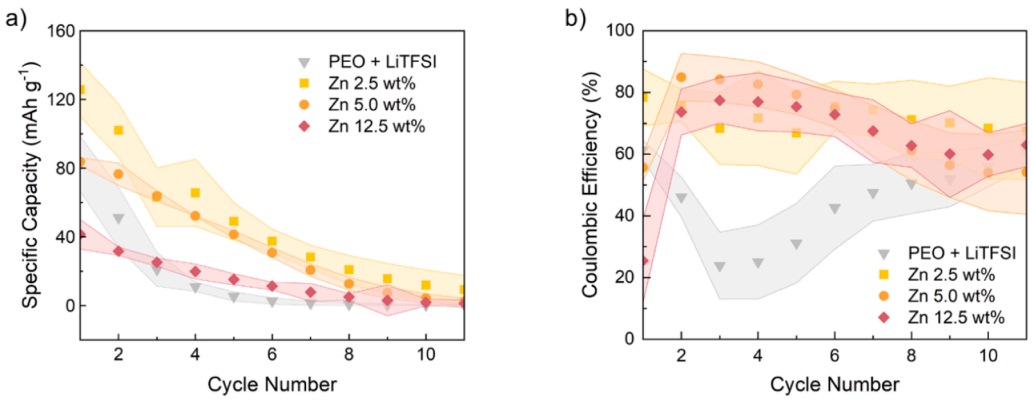


**Fig. 2.** a) Specific capacity and b) coulombic efficiency of anode-free batteries (Cu vs. LFP, N/*P*=0) with PEO:LiTFSI containing different amount of $Zn(OTf)_2$ (0, 2.5, 5.0 and 12.5 wt% respectively). Tests performed at 60 °C, 0.1 C (≈ 40 μA $cm^{-2}$), voltage interval 2.7 – 4.0 V. The shaded area represents the standard deviation.

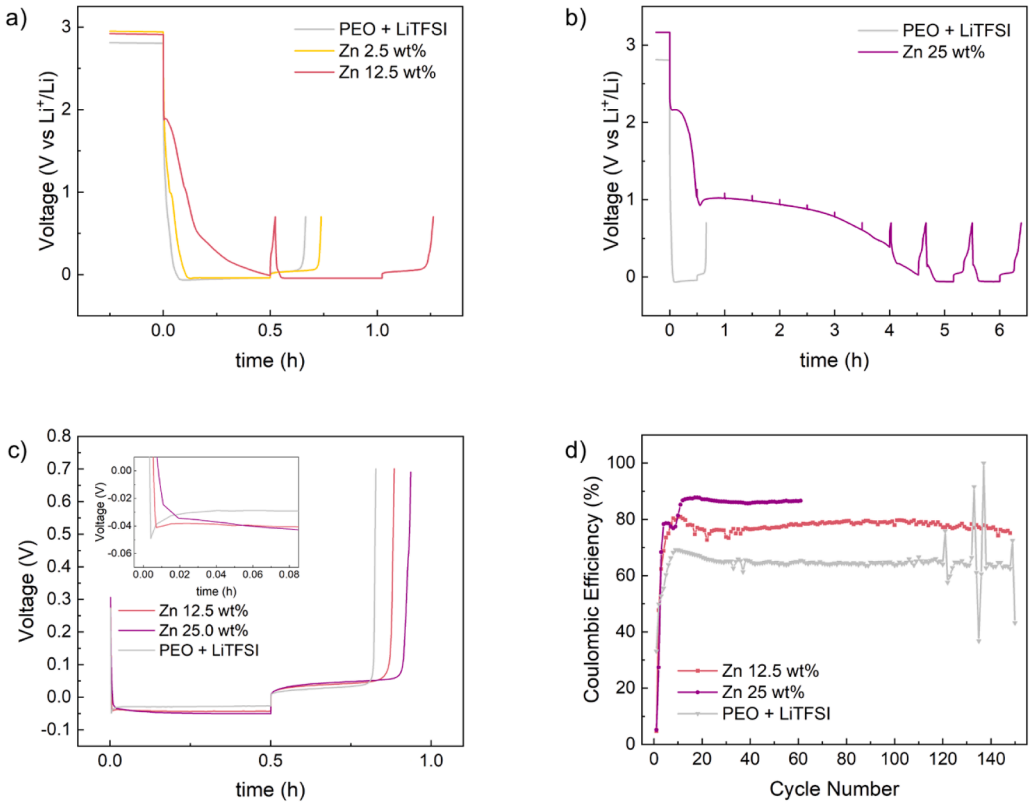


**Fig. 3.** Plating/stripping curves of Cu vs. Li with the SPEs in between with different amounts of Zn-salts. a, b) First cycle of the plating/stripping protocol. Plating capacity = 0.025 mA $cm^{-2}$; c) 20th cycle of plating/stripping protocol, inset showing the Li nucleation region; d) coulombic efficiency of plating/stripping tests. Current density = 0.05 mA $cm^{-2}$, *T*=60 °C.

information regarding the plating/stripping reaction. Furthermore, by increasing the amount of $Zn(OTf)_2$ to 25 wt%, an even higher coulombic efficiency, close to 90%, was achieved (see Fig. 3d), again highlighting the positive effect of the lithiophilic layer.

## 4. Conclusions

An innovative and practical strategy, exploiting the joint effect of lithiophilic metals and solid polymer electrolytes is here proposed to improve the efficiency of the Li-metal plating/stripping reaction for anode-free solid-state lithium metal batteries. To this end, lithiophilic Zn triflate was added to a conventional PEO-based SPE containing LiTFSI salt. The addition of secondary salt did not negatively affect the SPE properties, but instead contributed to an improvement of the specific capacity of an anode-free solid-state Cu||LFP battery. In particular, the specific capacity of the first cycle was increased from 82 mAh $g^{-1}$ to 126 mAh $g^{-1}$ and the capacity fading was reduced. Moreover, a plating/stripping protocol was implemented and the possibility to *in situ* deposit an interlayer of lithiophilic zinc metal on the Cu current collector during the very first cycle was demonstrated. Thereby, it was possible to facilitate the Li-metal deposition process and increase the coulombic efficiency up to 90% for the Zn-containing SPE. This is likely a direct consequence of the better nucleation of the Li-metal on top of the lithiophilic metal, reducing the formation of dendrites and dead lithium. These results propose a straightforward way to exploit lithiophilic metals by the direct addition to the SPE in the form of salts, and plating

them *in situ* during operation. For anode-free systems, this demonstrates the possibility to improve the critical efficiency and the reversibility of the Li-metal deposition process.

## CRediT authorship contribution statement

**Luca Bertoli:** Conceptualization, Methodology, Investigation, Writing – original draft. **Sophia Bloch:** Methodology, Investigation, Writing – review & editing. **Edvin Andersson:** Investigation, Writing – review & editing. **Luca Magagnin:** Writing – review & editing. **Daniel Brandell:** Writing – review & editing, Supervision, Funding acquisition. **Jonas Mindemark:** Methodology, Writing – review & editing, Supervision, Funding acquisition.

## Declaration of Competing Interest

The authors declare that they have no known competing financial interests or personal relationships that could have appeared to influence the work reported in this paper.

## Acknowledgments

This work was supported by the Swedish Foundation for Strategic Research (project SOLID ALiBI, grant no. 139501338), the ERC, grant no. 771777 FUN POLYSTORE, and STandUP for Energy. The authors would like to thank Isabell L. Johansson and Rassmus Andersson for the help in experimental work organization and DSC data acquisition.

## Supplementary materials

Supplementary material associated with this article can be found, in the online version, at doi:10.1016/j.electacta.2023.142874.

## References

[1] V. Etacheri, R. Marom, R. Elazari, G. Salitra, D. Aurbach, Challenges in the development of advanced Li-ion batteries: a review, Energy Environ. Sci. 4 (2011) 3243–3262, https://doi.org/10.1039/c1ee01598b.
[2] D. Deng, Li-ion batteries: basics, progress, and challenges, Energy Sci. Eng. 3 (2015) 385–418, https://doi.org/10.1002/ese3.95.
[3] Z. Xie, Z. Wu, X. An, X. Yue, J. Wang, A. Abudula, G. Guan, Anode-free rechargeable lithium metal batteries: progress and prospects, Energy Storage Mater. 32 (2020) 386–401, https://doi.org/10.1016/j.ensm.2020.07.004.
[4] Z.A. Ghazi, Z. Sun, C. Sun, F. Qi, B. An, F. Li, H.M. Cheng, Key aspects of lithium metal anodes for lithium metal batteries, Small 15 (2019), 1900687, https://doi.org/10.1002/smll.201900687.
[5] C.J. Huang, B. Thirumalraj, H.C. Tao, K.N. Shitaw, H. Sutiono, T.T. Hagos, T. T. Beyene, L.M. Kuo, C.C. Wang, S.H. Wu, W.N. Su, B.J. Hwang, Decoupling the origins of irreversible coulombic efficiency in anode-free lithium metal batteries, Nat. Commun. 12 (2021) 1–10, https://doi.org/10.1038/s41467-021-21683-6.
[6] S.S. Zhang, X. Fan, C. Wang, A tin-plated copper substrate for efficient cycling of lithium metal in an anode-free rechargeable lithium battery, Electrochim. Acta 258 (2017) 1201–1207, https://doi.org/10.1016/j.electacta.2017.11.175.
[7] Y. Tian, Y. An, C. Wei, H. Jiang, S. Xiong, J. Feng, Y. Qian, Recently advances and perspectives of anode-free rechargeable batteries, Nano Energy 78 (2020), 105344, https://doi.org/10.1016/j.nanoen.2020.105344.
[8] J. Qian, B.D. Adams, J. Zheng, W. Xu, W.A. Henderson, J. Wang, M.E. Bowden, S. Xu, J. Hu, J.G. Zhang, Anode-free rechargeable lithium metal batteries, Adv. Funct. Mater. 26 (2016) 7094–7102, https://doi.org/10.1002/adfm.201602353.
[9] A.J. Louli, A. Eldesoky, R. Weber, M. Genovese, M. Coon, J. DeGooyer, Z. Deng, R. T. White, J. Lee, T. Rodgers, R. Petibon, S. Hy, S.J.H. Cheng, J.R. Dahn, Diagnosing and correcting anode-free cell failure via electrolyte and morphological analysis, Nat Energy 5 (2020) 693–702, https://doi.org/10.1038/s41560-020-0668-8.
[10] S. Nanda, A. Gupta, A. Manthiram, Anode-free full cells: a pathway to high-energy density lithium-metal batteries, Adv. Energy Mater. 11 (2021), https://doi.org/10.1002/aenm.202000804, 2000804.
[11] S. Pyo, S. Ryu, Y.J. Gong, J. Cho, H. Yun, H. Kim, J. Lee, B. Min, Y. Choi, J. Yoo, Y. S. Kim, Lithiophilic wetting agent inducing interfacial fluorination for long-lifespan anode-free lithium metal batteries, Adv. Energy Mater. 13 (2023), 2203573, https://doi.org/10.1002/aenm.202203573.
[12] K.B. Hatzell, X.C. Chen, C.L. Cobb, N.P. Dasgupta, M.B. Dixit, L.E. Marbella, M. T. McDowell, P.P. Mukherjee, A. Verma, V. Viswanathan, A.S. Westover, W. G. Zeier, Challenges in lithium metal anodes for solid-state batteries, ACS Energy Lett. 5 (2020) 922–934, https://doi.org/10.1021/acsenergylett.9b02668.
[13] A. Hayashi, M. Tatsumisago, Sulfide-glass electrolytes for all-solid-state batteries. Encyclopedia of Glass Science, Technology, History, and Culture, Wiley, 2021, pp. 1125–1134, https://doi.org/10.1002/9781118801017.ch9.5.
[14] Q. Zhao, X. Liu, S. Stalin, K. Khan, L.A. Archer, Solid-state polymer electrolytes with in-built fast interfacial transport for secondary lithium batteries, Nat Energy 4 (2019) 365–373, https://doi.org/10.1038/s41560-019-0349-7.
[15] Y. Zhao, L. Wang, Y. Zhou, Z. Liang, N. Tavajohi, B. Li, T. Li, Solid polymer electrolytes with high conductivity and transference number of li ions for li-based rechargeable batteries, Adv. Sci. 8 (2021), https://doi.org/10.1002/advs.202003675, 2003675.
[16] L. Meabe, I. Aldalur, S. Lindberg, M. Arrese-Igor, M. Armand, M. Martinez-Ibañez, H. Zhang, Solid-state electrolytes for safe rechargeable lithium metal batteries: a strategic view, Mater. Futures (2023), https://doi.org/10.1088/2752-5724/accdf3.
[17] J. Qiu, X. Liu, R. Chen, Q. Li, Y. Wang, P. Chen, L. Gan, S.J. Lee, D. Nordlund, Y. Liu, X. Yu, X. Bai, H. Li, L. Chen, Enabling stable cycling of 4.2V high-voltage all-solid-state batteries with PEO-based solid electrolyte, Adv. Funct. Mater. 30 (2020), https://doi.org/10.1002/adfm.201909392.
[18] J.F. Snyder, R.H. Carter, E.D. Wetzel, Electrochemical and mechanical behavior in mechanically robust solid polymer electrolytes for use in multifunctional structural batteries, Chem. Mater. 19 (2007) 3793–3801, https://doi.org/10.1021/cm070213o.
[19] J. Mindemark, B. Sun, E. Törmä, D. Brandell, High-performance solid polymer electrolytes for lithium batteries operational at ambient temperature, J. Power Sources 298 (2015) 166–170, https://doi.org/10.1016/j.jpowsour.2015.08.035.
[20] I.L. Johansson, C. Sångeland, T. Uemiya, F. Iwasaki, M. Yoshizawa-Fujita, D. Brandell, J. Mindemark, Improving the electrochemical stability of a polyester-polycarbonate solid polymer electrolyte by zwitterionic additives, ACS Appl. Energy Mater. 5 (2022) 10002–10012, https://doi.org/10.1021/acsaem.2c01641.
[21] T. Krauskopf, H. Hartmann, W.G. Zeier, J. Janek, Toward a fundamental understanding of the lithium metal anode in solid-state batteries - an electrochemo-mechanical study on the garnet-type solid electrolyte Li 6.25 Al 0.25 La 3 Zr 2 O 12, ACS Appl. Mater. Interfaces 11 (2019) 14463–14477, https://doi.org/10.1021/acsami.9b02537.
[22] E.K.W. Andersson, C. Sångeland, E. Berggren, F.O.L. Johansson, D. Kühn, A. Lindblad, J. Mindemark, M. Hahlin, Early-stage decomposition of solid polymer electrolytes in Li-metal batteries, J. Mater. Chem. A Mater. 9 (2021) 22462–22471, https://doi.org/10.1039/d1ta05015j.
[23] M.N. Obrovac, V.L. Chevrier, Alloy negative electrodes for Li-ion batteries, Chem. Rev. 114 (2014) 11444–11502, https://doi.org/10.1021/cr500207g.
[24] E. Cha, J.H. Yun, R. Ponraj, D.K. Kim, A mechanistic review of lithiophilic materials: resolving lithium dendrites and advancing lithium metal-based batteries, Mater. Chem. Front. 5 (2021) 6294–6314, https://doi.org/10.1039/d1qm00579k.
[25] X.R. Chen, X. Chen, C. Yan, X.Q. Zhang, Q. Zhang, J.Q. Huang, Role of lithiophilic metal sites in lithium metal anodes, Energy Fuels 35 (2021) 12746–12752, https://doi.org/10.1021/acs.energyfuels.1c01602.
[26] J. Deng, Y. Wang, S. Qu, Y. Liu, W. Zou, F. Zhou, A. Zhou, J. Li, Fast Li+ transport of Li−Zn alloy protective layer enabling excellent electrochemical performance of Li metal anode, Batter Supercaps 4 (2021) 140–145, https://doi.org/10.1002/batt.202000125.
[27] N. Delaporte, A. Perea, S. Collin-Martin, M. Léonard, J. Matton, V. Gariepy, H. Demers, D. Clément, E. Rivard, A. Vijh, High performance lithium metal anode with a nanolayer of LiZn alloy for all-solid-state batteries, Batter Supercaps 5 (2022), e202200245, https://doi.org/10.1002/batt.202200245.
[28] M. Zhu, K. Xu, D. Li, T. Xu, W. Sun, Y. Zhu, Y. Qian, Guiding smooth Li plating and stripping by a spherical island model for lithium metal anodes, ACS Appl. Mater. Interfaces 12 (2020) 38098–38105, https://doi.org/10.1021/acsami.0c09430.
[29] S. Cui, P. Zhai, W. Yang, Y. Wei, J. Xiao, L. Deng, Y. Gong, Large-scale modification of commercial copper foil with lithiophilic metal layer for Li metal battery, Small 16 (2020), 1905620, https://doi.org/10.1002/smll.201905620.
[30] Y. Liu, D. Gao, H. Xiang, X. Feng, Y. Yu, Research progress on copper-based current collector for lithium metal batteries, Energy Fuels 35 (2021) 12921–12937, https://doi.org/10.1021/acs.energyfuels.1c02008.
[31] M.C. Stan, J. Becking, A. Kolesnikov, B. Wankmiller, J.E. Frerichs, M.R. Hansen, P. Bieker, M. Kolek, M. Winter, Sputter coating of lithium metal electrodes with lithiophilic metals for homogeneous and reversible lithium electrodeposition and electrodissolution, Mater. Today 39 (2020) 137–145, https://doi.org/10.1016/j.mattod.2020.04.002.
[32] Z. Zuo, L. Zhuang, J. Xu, Y. Shi, C. Su, P. Lian, B. Tian, Lithiophilic silver coating on lithium metal surface for inhibiting lithium dendrites, Front. Chem. 8 (2020) 109, https://doi.org/10.3389/fchem.2020.00109.
[33] A. Kato, A. Hayashi, M. Tatsumisago, Enhancing utilization of lithium metal electrodes in all-solid-state batteries by interface modification with gold thin films, J. Power Sources 309 (2016) 27–32, https://doi.org/10.1016/j.jpowsour.2016.01.068.
[34] S. Liu, X. Zhang, R. Li, L. Gao, J. Luo, Dendrite-free Li metal anode by lowering deposition interface energy with Cu99Zn alloy coating, Energy Storage Mater. 14 (2018) 143–148, https://doi.org/10.1016/j.ensm.2018.03.004.
[35] Y.G. Lee, S. Fujiki, C. Jung, N. Suzuki, N. Yashiro, R. Omoda, D.S. Ko, T. Shiratsuchi, T. Sugimoto, S. Ryu, J.H. Ku, T. Watanabe, Y. Park, Y. Aihara, D. Im, I.T. Han, High-energy long-cycling all-solid-state lithium metal batteries enabled by silver–carbon composite anodes, Nat Energy 5 (2020) 299–308, https://doi.org/10.1038/s41560-020-0575-z.
[36] L.Z. Fan, H. He, C.W. Nan, Tailoring inorganic–polymer composites for the mass production of solid-state batteries, Nat. Rev. Mater. 6 (2021) 1003–1019, https://doi.org/10.1038/s41578-021-00320-0.

[37] L. Yue, J. Ma, J. Zhang, J. Zhao, S. Dong, Z. Liu, G. Cui, L. Chen, All solid-state polymer electrolytes for high-performance lithium ion batteries, Energy Storage Mater. 5 (2016) 139–164, https://doi.org/10.1016/j.ensm.2016.07.003.
[38] J. Mindemark, E. Törmä, B. Sun, D. Brandell, Copolymers of trimethylene carbonate and ε-caprolactone as electrolytes for lithium-ion batteries, Polymer 63 (2015) 91–98, https://doi.org/10.1016/j.polymer.2015.02.052.
[39] M.I.D. Rosero, N.M.J. Meneses, R.U. Kaffure, Thermal properties of composite polymer electrolytes poly(ethylene oxide)/sodium trifluoroacetate/aluminum oxide (PEO)10CF3COONa + x wt.% Al2O3, Materials 12 (2019) 1464, https://doi.org/10.3390/ma12091464.
[40] S. Klongkan, J. Pumchusak, Effects of nano alumina and plasticizers on morphology, ionic conductivity, thermal and mechanical properties of PEO-LiCF3SO3 Solid Polymer Electrolyte, Electrochim. Acta 161 (2015) 171–176, https://doi.org/10.1016/j.electacta.2015.02.074.
[41] R. Younesi, G.M. Veith, P. Johansson, K. Edström, T. Vegge, Lithium salts for advanced lithium batteries: li-metal, Li-O2, and Li-S, Energy Environ. Sci. 8 (2015) 1905–1922, https://doi.org/10.1039/c5ee01215e.
[42] L. Qiao, U. Oteo, M. Martinez-Ibañez, A. Santiago, R. Cid, E. Sanchez-Diez, E. Lobato, L. Meabe, M. Armand, H. Zhang, Stable non-corrosive sulfonimide salt for 4-V-class lithium metal batteries, Nat. Mater. 21 (2022) 455–462, https://doi.org/10.1038/s41563-021-01190-1.
[43] T.M. Hagos, H.K. Bezabh, C.J. Huang, S.K. Jiang, W.N. Su, B.J. Hwang, A powerful protocol based on anode-free cells combined with various analytical techniques, Acc. Chem. Res. 54 (2021) 59, https://doi.org/10.1021/acs.accounts.1c00528.